JCTC Journal of Chemical Theory and Computation

ARTICLE

pubs.acs.org/JCTC

Time-Reversible Velocity Predictors for Verlet Integration with Velocity-Dependent Right-Hand Side

Jiří Kolafa*,† and Martin Lísal‡,§

†Department of Physical Chemistry, Institute of Chemical Technology, Prague, Technická 5, 166 28 Praha 6, Czech Republic

‡E. Hála Laboratory of Thermodynamics, Institute of Chemical Process Fundamentals of the ASCR, v. v. i., 165 02 Prague 6, Czech Republic

§Department of Physics, J. E. Purkinje University, 400 96 Ústí n. Lab., Czech Republic

Supporting Information

ABSTRACT: Time-reversible velocity predictors (TRVPs) with increasing orders of the time-reversibility error are developed to be used with the Verlet integrator for equations of motion with the right-hand side depending on velocities. The method performs outside a possible SHAKE algorithm to constrain bond lengths and does not require repeated SHAKE iterations nor RATTLE. We have tested the TRVPs with the Nosé−Hoover thermostat on four model systems (coupled harmonic and anharmonic oscillators, liquid argon, SPC/E water, and a small peptide), comparing them to the Gear integrator with the Lagrangian formulation of constraint dynamics, the Martyna, Tuckerman, Tobias, and Klein (MTTK) method, and the velocity iteration method. The TRVP method performs similarly to the iteration method. In addition, we discuss three methodology improvements: (i) We tested several formulas for the kinetic energy compatible with the Verlet/SHAKE algorithm and found that the leapfrog velocities are usually the best; (ii) we proposed two modifications of the MTTK method; and (iii) we suggest that thermostats directly controlling the translational kinetic temperature may give more accurate values of some thermodynamic quantities.

1. INTRODUCTION

The Newton equations of motion for atomistic systems relate accelerations to forces which are functions of positions only, not velocities. Although many smart methods have been proposed, a great deal of existing molecular dynamics (MD) code relies on the simplest Verlet integrator.[1,2]

Extended Lagrangian methods, as the Nosé−Hoover thermostat and Andersen barostat, add a velocity-dependent term to the equations of motion; hence, using the Verlet integrator and its clones (leapfrog, velocity Verlet, Beeman) directly is no longer possible because the velocities at time t are known after the forces at time t have been evaluated. Alternative integration methods include the predictor−corrector methods,[3] of these the Gear integrators[4] are most popular. The integrators, based on the Trotter decomposition of the Liouville operator,[5] may be viewed as an extension of the Verlet integrator and may be combined with SHAKE and RATTLE. If one wants to adhere to the Verlet scheme, either iterations can be used to obtain the velocities or some approximation of these.[6]

The time reversibility error leading to a drift in the total energy (Hamiltonian) which should be conserved is worst in the Gear methods. The MTTK method[5] (see Section 2.7.3) is time reversible, although not symplectic: There is no drift in the total energy, but the mean quadratic error grows as the square root of time. In the iteration methods, there is a small drift decreasing with an increasing number of iterations.

In this paper we propose a velocity predictor so that iterations can be avoided. The predictor is of the second order (as the Verlet method), and the main requirement for its construction is time reversibility. During extensive testing of the methods, we found several improvements of the simulation methodology.

2. THEORY

2.1. Notation and Kinetic Temperature. Let us consider a system of N atoms with masses m_i, positions described by vectors $\vec{r}_i$, and velocities by $\dot{\vec{r}}_i$, $i = 1, ..., N$. The force acting on particle i is denoted as $\vec{f}_i$. The kinetic temperature is then defined by formula:

$$T_{\mathrm{kin}} = \frac{1}{fk}\sum_{i=1}^{N} m_i \dot{\vec{r}}_i^{\,2} \tag{1}$$

where k is the Boltzmann constant, and $f = Nd + f_\xi - f_c$ is the number of degrees of freedom. In this formula, d denotes the space dimensionality, f_ξ the number of additional degrees of freedom with quadratic term for the kinetic energy, and f_c denotes the number of constraints, typically bond lengths and conserved quantities (momentum, angular momentum, and also total energy).

2.2. Nosé−Hoover Thermostat. We use the Nosé−Hoover thermostat as a model of equations of motion with the right-hand side containing velocities. The equations of motion of this system at temperature T are[7,8]

$$\ddot{\vec{r}}_i = \frac{\vec{f}_i}{m_i} - \dot{\vec{r}}_i\dot{\xi} \tag{2}$$

$$\ddot{\xi} = \frac{1}{\tau^2}\left(\frac{T_{\mathrm{kin}}}{T} - 1\right) \tag{3}$$

Received: February 15, 2011
Published: August 31, 2011

Here, ξ is the additional dynamic variable and τ the typical correlation time of the thermostat. The particle accelerations depend on all velocities (including $\dot{\xi}$ which we consider a velocity, although it is not a velocity in the original Lagrangian formalism[7]), whereas the acceleration of the additional variable depends on the real degrees of freedom only. The equations of the Andersen barostat[1,2] (not considered here) have the same structure.

During integration the following total energy (derived from the Hamiltonian[7]) is conserved

$$E_{\mathrm{NH}} = E_{\mathrm{kin}} + E_{\mathrm{pot}} + fkT\left(\xi + \frac{\tau^2\dot{\xi}2}{2}\right) \tag{4}$$

where E_{kin} is the kinetic energy and E_{pot} the potential (configurational) energy.

2.3. Verlet Method. The Verlet method for eqs 2 and 3 is respectively

$$\vec{r}_i(t+h) = 2\vec{r}_i(t) - \vec{r}_i(t-h) + \left[\frac{\vec{f}_i(t)}{m_i} - \dot{\vec{r}}_i(t)\dot{\xi}(t)\right]h^2 \tag{5}$$

$$\xi(t+h) = 2\xi(t) - \xi(t-h) + \frac{1}{\tau^2}\left[\frac{T_{\mathrm{kin}}(t)}{T} - 1\right]h^2 \tag{6}$$

where h is the time step. Various approximations for the unknown velocities $\dot{\vec{r}}_i(t)$ and $\dot{\xi}(t)$ as well as the kinetic temperature $T_{\mathrm{kin}}(t)$ (depending on the velocities) will be discussed below.

The Verlet method can be rewritten in the leapfrog form using definition:

$$\dot{q}(t+h/2) = \frac{q(t+h) - q(t)}{h} \tag{7}$$

where q stands for any coordinate component or ξ. It may be even advantageous in a computer code to use difference $q(t+h) - q(t)$ instead of $\dot{q}(t+h/2)$. All these variants yield identical trajectories and need not be distinguished, provided that eq 7 is treated as a formal definition of symbol $\dot{q}(t+h/2)$ (which approximates the velocity at time $t+h/2$ up to the order of $\mathcal{O}(h^2)$).

2.4. Time-Reversible Velocity Predictor. We propose to calculate the unknown velocities $\dot{q}^p(t)$ from the knowledge of the history (previous positions) by the following predictor:

$$\dot{q}^p(t) = \frac{1}{h}\sum_{i=0}^{k+1} A_i q(t-ih) \tag{8}$$

where k stands for the (additional) predictor length. For $k = 0$ the predictor uses only information known within the Verlet algorithm at time t, namely $q(t)$ and $q(t-h)$.

To determine constants A_i, $i = 0, \ldots, k+1$, we will use the method described elsewhere.[9] Let us Taylor expand the right-hand side of eq 8:

$$\sum_{i=0}^{k+1} A_i q(t-ih) = \frac{1}{j!}\sum_{j=0}^{\infty} X_j q^{(j)} h^j$$

where

$$X_j = \sum_{i=0}^{k+1} (-i)^j A_i$$

Equation 8 should give the velocity $\dot{q}^p(t)$ correct up to the second order (the order of the Verlet method). The following three equations must be thus satisfied

$$X_0 = \sum_{i=0}^{k+1} A_i = 0 \tag{9}$$

$$X_1 = -\sum_{i=0}^{k+1} iA_i = 1 \tag{10}$$

$$X_2 = \sum_{i=0}^{k+1} i^2 A_i = 0 \tag{11}$$

There is no solution for $k = 0$, therefore the minimum predictor length is $k = 1$. The first error term in eq 8 is then X_3h^2; it is even and therefore it does not cause time irreversibility. The next term, X_4h^3, causes time irreversibility of the third order $\mathcal{O}(h^3)$; it means that running a simulation with doubled time step multiplies the energy drift eight times.

If we consider $k > 1$, we can achieve a better time reversibility by nullifying the terms at odd powers of h:

$$X_{2j} = \sum_{i=0}^{k+1} i^{2j} A_i = 0, \qquad j = 1, 2, \ldots, k \tag{12}$$

The solution of eqs 9−12 is

$$\begin{aligned} A_0 &= \frac{2k+1}{k+1} \\ A_1 &= -2(2k+1)\frac{1}{k+2} \\ A_2 &= +2(2k+1)\frac{k}{(k+2)(k+3)} \\ A_3 &= -2(2k+1)\frac{k(k-1)}{(k+2)(k+3)(k+4)} \\ &\vdots \end{aligned}$$

or in a compact form

$$A_i = (-1)^i(1-\delta_{0i}/2)\binom{2k+2}{k+1-i}\Big/\binom{2k}{k}$$

where δ stands for the Kronecker delta.

2.4.1. Proof. To prove the above statement, let us first consider expressions for X_{2j}, $j = 0,1, \ldots, k$. They are composed of terms $A_i i^{2j}$, $i > 0$, which we write as

$$A_i i^{2j} = \frac{1}{2}[A_i(-i)^{2j} + A_i(+i)^{2j}]$$

The equation for X_{2j}, $j > 0$, then becomes

$$\begin{aligned} 2\binom{2k}{k}(-1)^{k+1}X_{2j} = &+\binom{2k+2}{0}(-k-1)^{2j} \\ &-\binom{2k+2}{1}(-k)^{2j} + \binom{2k+2}{2}(-k+1)^{2j} \\ &-\cdots\binom{2k+2}{2k+2}(k+1)^{2j} \end{aligned} \tag{13}$$

This is the operator of the $(2k+2)$-th difference applied to function $f(j) = (j-n-1)^{2j}$, and therefore the result is 0 for $2k+2 > 2j$, i.e., $j \le k$.[3] (The difference operator is defined by $\Delta f(j) = f(j) - f(j-1)$. A degree of a polynomial is decreased by one by

applying this operator. The sum in eq 13 then equals $\Delta^{2k+2}f(j)$ because the powers of the difference operator contain binomial coefficients with alternating signs, as can be shown by using the Pascal triangle.)

It remains to calculate X_1. After inserting for A_i, eq 10 becomes

$$\begin{aligned}\binom{2k}{k}X_1 &= \binom{2k}{k} \\ &= \binom{2k+2}{k} - 2\binom{2k+2}{k-1} \\ &\quad + 3\binom{2k+2}{k-3} - + \cdots \end{aligned} \tag{14}$$

To prove it, we recursively expand the binomial coefficient:

$$\begin{aligned}\binom{2k}{k} &= \binom{2k+1}{k} - \binom{2k}{k-1} \\ &= \binom{2k+1}{k} - \binom{2k+1}{k-1} + \binom{2k}{k-2} \\ &\vdots \\ &= \binom{2k+1}{k} - \binom{2k+1}{k-1} + \binom{2k+1}{k-2} \\ &\quad - + \ldots \end{aligned}$$

and then apply the same recursive expansion to every term in the last expression.

2.4.2. Final formula for TRVPs. It may be useful to express $\dot{q}^p(t)$ using the first differences. The advantages include smaller rounding errors and easier conversion to the Gear-type methods. The algorithm is then closer to the leapfrog form:

$$h\dot{q}^{\mathrm{PR}}(t) = \sum_{i=0}^{k} B_i[q(t-ih) - q(t-[i+1]h)] \tag{15}$$

It holds $B_0 = A_0$ and

$$B_j = (-1)^j(2k+1)\frac{k(k-1)\cdots(k+1-j)}{(k+1)(k+2)\cdots(k+1+j)}$$

or recursively

$$B_0 = \frac{2k+1}{k+1} \tag{16}$$

$$B_j = -B_{j-1} \times \frac{k+1-j}{k+1+j}, \qquad j>0 \tag{17}$$

which can be easily coded.

The drift in the total energy is of the order of h^{2k+1}.

2.5. Velocity Estimators and Kinetic Temperature. Several approximations of velocities can be used to calculate the kinetic temperature, eq 1. The simplest possibility is the difference formula which is equivalent to the so-called velocity Verlet (VV) algorithm:

$$\begin{aligned}\dot{\vec{r}}_i^{\,\mathrm{VV}}(t) &= \frac{\dot{\vec{r}}_i(t-h/2) + \dot{\vec{r}}_i(t+h/2)}{2} \\ &= \frac{\vec{r}_i(t+h) - \vec{r}_i(t-h)}{2h} \end{aligned} \tag{18}$$

The "harmonic approximation" (HA):

$$\begin{aligned}\dot{\vec{r}}_i^{\,\mathrm{HA}}(t)^2 &= \dot{\vec{r}}_i(t-h/2)\cdot\dot{\vec{r}}_i(t+h/2) \\ &= \frac{[\vec{r}_i(t+h) - \vec{r}_i(t)]\cdot[\vec{r}_i(t) - \vec{r}_i(t-h)]}{h^2} \end{aligned} \tag{19}$$

gives exactly constant total energy when the Verlet method is applied to a harmonic oscillator.

The "leap-frog approximation" (LF) makes an average of the approximated kinetic energies at midpoints:

$$\begin{aligned}\dot{\vec{r}}_i^{\,\mathrm{LF}}(t)^2 &= \frac{\dot{\vec{r}}_i(t-h/2)^2 + \dot{\vec{r}}_i(t+h/2)^2}{2} \\ &= \left[\frac{\vec{r}_i(t+h) - \vec{r}_i(t)}{h}\right]^2 + \left[\frac{\vec{r}_i(t) - \vec{r}_i(t-h)}{h}\right]^2 \end{aligned} \tag{20}$$

Finally, one can use the predicted velocities, $\dot{\vec{r}}_i^{\,\mathrm{PR}}(t)$, see eq 15, to calculate the kinetic temperature. This choice, denoted hereafter as PR, is independent of the particular form of the right-hand side. In contrast, options VV, HA, and LF require a particular right-hand side, eqs 2 and 3 or similar, as algorithmized below.

2.6. TRVP Algorithm. The proposed method can be easily combined with the SHAKE algorithm to maintain constraints (typically bond lengths). It can be written in several equivalent forms. Because of reduced numerical errors, we store the history of differences $q(t) - q(t-h)$, $q(t-h) - q(t-2h)$, etc., rather than the positions. One step from t to $t+h$ of the combined predicted velocity Nosé–Hoover Verlet integration with optional SHAKE method is then summarized below:

(1) Calculate the potential energy and forces $\vec{f}_i(t)$ from known positions $\vec{r}_i(t)$.
(2) Predict velocities $\dot{q}$ ($q = \{\vec{r}_i, \xi\}$) from known history $q(t) - q(t-h), q(t-h) - q(t-2h), \ldots, q(t-kh) - q(t-[k+1]h)$, using eqs 15, 16, and 17.
(3) Perform one step of the Verlet method, eq 5, to get $\vec{r}_i(t+h)$.
(4) Run the SHAKE algorithm; $\vec{r}_i(t+h)$ are modified.
(5) Calculate new differences $\vec{r}_i(t+h) - \vec{r}_i(t)$.
(6) Calculate the kinetic temperature by one of four available eqs 18–20 and 15; below we will recommend eq 20.
(7) Perform one step of the Verlet method, eq 6, for ξ to get $\xi(t+h)$.
(8) Calculate the total energy at time t.
(9) Advance time, $t := t+h$.

The algorithm does not need iterations (except those inside SHAKE). At the integration start the history needed for Step 2 is not known, and shorter predictors ($k = 0,1,2,\ldots$) must be used. Since a typical MD run includes equilibration, this will rarely be a problem.

2.7. Other Methods. We compare the proposed TRVP method with several known methods.

2.7.1. Gear Integration and Lagrangian Constraint Dynamics. The Gear integration method[1,4] is based on storing the history in the form of a vector of higher derivatives at time t, $(q(t), h\dot{q}(t), (h^2/2)\ddot{q}(t), \ldots)$, from which the positions and velocities at time $t+h$ are predicted by the Taylor expansion. The integration step thus has an easy access to velocities, and the method is straightforward unless constraints are to be satisfied.

For systems with constrained bonds we use the Lagrangian formulation of the constrained dynamics.[10] It is based on evaluation of the constraint forces by Lagrange multipliers; the set of linear equations is solved by the conjugate gradient method.[11] Since the constrains are satisfied only up to the order of the method and rounding errors, they are corrected by the same method at every step.

2.7.2. Verlet with Iterated Velocities. As already mentioned, the Verlet-family integrators suffer from a chicken-or-egg problem: The velocities needed in an integration step are known after the integration step is finished, i.e., the velocities are given implicitly by a set of equations. These equations can be solved by iterations.[6] The algorithm reads as[12]

(1) Calculate the potential energy and forces $\vec{f}_i(t)$ from known positions $\vec{r}_i(t)$.
(2) Initial approximation:
Version 1: $\dot{\vec{r}}_i(t) := [\vec{r}_i(t) - \vec{r}_i(t-h)]/h$, $\dot{\xi}(t) := [\xi(t) - \xi(t-h)]/h$.
Version 2: $\dot{\vec{r}}_i(t) := 0$, $\dot{\xi}(t) := 0$.
(3) Repeat the following loop:
(a) Perform one step of the Verlet method, eq 5, to get $\vec{r}_i(t+h)$ (using velocities $\dot{\vec{r}}_i(t)$).
(b) Run the SHAKE algorithm; $\vec{r}_i(t+h)$ are modified. (Omitted in the first iteration of Version 2.)
(c) Calculate new velocities $\dot{\vec{r}}_i(t) := [\vec{r}_i(t+h) - \vec{r}_i(t-h)]/(2h)$.
(d) Calculate the kinetic temperature by one of eqs 18−20.
(e) Perform one step of the Verlet method, eq 6, to get $\xi(t+h)$.
(f) Calculate the new velocity $\dot{\xi}(t) := [\xi(t+h) - \xi(t-h)]/(2h)$.
(4) Calculate the total energy at time t.
(5) Advance time, $t := t + h$.

The number of iterations (Step 3) may be either fixed or controlled by a predefined accuracy of the velocities. Note that the forces are calculated once per step, however, SHAKE iterations must be repeated (although less iterations are then needed). One pass (iteration) of Version 1 is equivalent to TRVP ($k = 0$), which is not accurate enough.

2.7.3. MTTK Method. A smart method keeping the Verlet scheme for positions but replacing the integrator of ξ has been proposed.[5] The algorithm is[12]

(1) $\dot{\xi}(t+h/4) := \dot{\xi}(t) + (h/4)a(t)$, where $a(t) = [T_{\mathrm{kin}}(t)/T - 1]/\tau^2$.
(2) $\dot{\vec{r}}^{\,*}_i(t) := \dot{\vec{r}}_i(t)\,\mathrm{sym}[-(h/2)\dot{\xi}(t+h/4)]$.
(3) $\xi(t+h/2) := \xi(t+h/4) + (h/4)a^*(t)$, where $a^*(t)$ is calculated from the velocities calculated in the previous step.
(4) $\dot{\vec{r}}_i(t+h/2) := \dot{\vec{r}}_i(t) + (h/2)\vec{f}_i/m_i$.
(5) $\vec{r}_i(t+h) := \vec{r}_i(t) + h\dot{\vec{r}}_i(t+h/2)$.
(6) Run (the first part of) the RATTLE algorithm.
(7) Calculate forces $\vec{f}_i(t+h)$ from $\vec{r}_i(t+h)$.
(8) $\dot{\vec{r}}_i(t+h) := \dot{\vec{r}}_i(t+h/2) + (h/2)\vec{f}_i(t+h)/m_i$.
(9) Run (the second part of) the RATTLE algorithm.
(10) $\dot{\xi}(t+3h/4) := \dot{\xi}(t+h/2) + (h/4)a(t+h)$, where $a(t+h)$ is calculated from the RATTLE velocities.
(11) $\dot{\vec{r}}^{\,*}_i(t+h) := \dot{\vec{r}}_i(t+h)/\mathrm{sym}[(h/2)\dot{\xi}(t+3h/4)]$.
(12) $\xi(t+h) := \xi(t+3h/4) + (h/4)a^*(t+h)$, where $a^*(t+h)$ is calculated from the velocities calculated in the previous step.

In the original work the function

$$\mathrm{sym}(x) = \exp(x) \tag{21}$$

is derived by the Trotter decomposition of the Liouville operator. We will denote this version by letter e.

2.7.4. Modification of MTTK Method. It follows from reading the MTTK algorithm in the bottom-up direction that the method is time reversible for any function $\mathrm{sym}(x)$. However, $\mathrm{sym}(x) \approx 1 + x$ is required to maintain the order of the method. We thus propose two computationally less expensive functions:

$$\mathrm{sym}_+(x) = 1 + x \tag{22}$$

$$\mathrm{sym}_-(x) = 1/(1-x) \tag{23}$$

The speed gain is marginal for large atomic systems but may be significant for simple enough systems. We will denote these versions by symbols + and −, respectively.

2.7.5. Berendsen Thermostat. The Berendsen (friction) thermostat[1,2] is used for comparison. The equations of motion are modified by a friction term:[11]

$$\ddot{\vec{r}}_i = \frac{\vec{f}_i}{m_i} - \frac{\ln(T_{\mathrm{kin}}/T)}{2\tau}\dot{\vec{r}}_i$$

In a simulation of a dilute system (ideal gas), the temperature relaxes to the thermostat value T exponentially with the correlation time of τ. In the simplest implementation to the Verlet scheme, velocities $\dot{\vec{r}}_i(t+h/2)$ are multiplied by factor $\exp[-\ln(T_{\mathrm{kin}}(t)/T)h/(2\tau)]$ after every step.

2.8. Simulation Details. *2.8.1. Potential Cutoff.* In molecular models of argon and water we use a smoothly truncated Lennard-Jones potential given by the formula:[11]

$$u_{\mathrm{LJ}}(r) \approx \begin{cases} 4\varepsilon[(\sigma/r)^{12} - (\sigma/r)^6] & \text{for } r < C_1 \\ A(r^2 - C_2^2)^2 & \text{for } C_1 < r < C_2 \\ 0 & \text{for } C_2 < r \end{cases}$$

where C_1 and A are calculated from the cutoff C_2 so that both the potential and the forces are continuous. Standard cutoff corrections for the potential energy and pressure are calculated using the usual assumption that the radial distribution function is unity beyond C_1.

The SPC/E water model[13] contains partial charges. In order to avoid additional errors inherent to more sophisticated methods (Ewald summation, reaction field) and also to gain speed, we use a simple truncated formula[14] to approximate the electrostatic forces. The $1/r$ term in the Coulomb energy is replaced by

$$\frac{1}{r} \approx \begin{cases} 1/r - s & \text{for } r < C_1 \\ (r - C_2)^3(A + Br) & \text{for } C_1 < r < C_2 \\ 0 & \text{for } C_2 < r \end{cases} \tag{24}$$

where $C_1 = 0.7C_2$. The shift s and parameters A and B are determined so that the potential, forces, and the derivative of forces are continuous. The electrostatic force is thus neglected beyond the cutoff, shifted at short separations, and smoothly interpolated in between.

2.8.2. Mechanical Quantities. The averaged potential energy, E_{pot}, also called residual internal energy, can be regarded as the most important and simplest mechanical quantity.

The second mechanical quantity of interest is pressure, which is calculated from the virial of force. This is straightforward for liquid argon. For constrained models there are two possibilities. To evaluate the instantaneous pressure in the TRVP, Gear, and Berendsen methods, we use the atom-based formula:

$$P = \frac{1}{3V}(2E_{\mathrm{kin}} + \sum_{i<j} r_{ij} f_{ij}) \tag{25}$$

where we use notation $|\vec{r}| = r$. The sum runs over all interacting pairs of particles (with the distance calculated by the nearest image convention). Forces f_{ij} include the constraint forces calculated within the SHAKE procedure or given by Lagrange multipliers. This pressure thus depends on velocities.

To evaluate the pressure in the iteration and MTTK methods, we use the molecule-based formula:

$$P = \frac{1}{3V}\left[2E_{\mathrm{tr}} + \sum_{n<m}\sum_{i}\sum_{j}\frac{(\vec{R}_{nm}\cdot\vec{r}_{ni,mj})}{R_{nm}} f_{ni,mj}\right] \tag{26}$$

where $\vec{R}_n$ is the position of a reference point (for water we use oxygen) in molecule n. Position of atom i at molecule n is denoted as $\vec{r}_{ni}$ and $\vec{r}_{ni,mj} = \vec{r}_{mj} - \vec{r}_{ni}$ (with the nearest-image rule). Instead of the total kinetic energy, only the translational part is used

$$E_{\mathrm{tr}} = \frac{1}{2}\sum_{n=1}^{N} M_n V_n^2$$

where M_n (V_n) is the mass (velocity) of the center-of-mass of molecule n. Both methods give the same results up to the order of the integrator.

The virial of electrostatic forces is the same (but sign) as the electrostatic energy. However, if the electrostatic forces are approximated by eq 24, this relation is only approximate. We use a direct evaluation of the virial because it has been shown[14] that it gives a better approximation of the true pressure.

2.8.3. Control Quantities. The drift in the total energy E_{NH}, eq 4, is an auxiliary control quantity which is sensitive to time irreversibility. We calculate it by linear regression from the $E_{\mathrm{NH}}(t)$ dependence.

The quality of the canonical distribution of particle velocities can be generally monitored by moments. All odd moments are zero because of symmetry. The second moment, variance of velocity (averaged over particles), is proportional to the kinetic temperature. The next nonzero moment is the kurtosis:

$$\mathrm{kurtosis} = \frac{\langle v^4\rangle}{\langle v^2\rangle^2} - 3 \tag{27}$$

Here v represents any component of the velocity and $\langle\cdot\rangle$ includes averaging over all equivalent degrees of freedom. The kurtosis is zero for the Gaussian distribution.

Since we use different approximations of velocity, eqs 15 and 18−20, it is "natural" to use the same definition also for kurtosis. This is easy because only a squared velocity appears in eq 27. For some purposes (e.g., the velocity autocorrelation function), the velocity versions HA and LF are not directly applicable, and therefore either the simple leapfrog $\vec{r}(t - h/2)$ or VV must be used instead of the "natural" definition. It then makes sense to determine kurtosis also for these alternate definitions.

The variance of the kinetic temperature is an important quantity related to heat capacity. Unlike kurtosis, which is a single-particle property, the variance of temperature depends on the whole configuration. From the Maxwell−Boltzmann distribution one can easily calculate that

$$\mathrm{var}T_{\mathrm{kin}} = \frac{2T^2}{f} \tag{28}$$

It is important in simulations of complex systems that both slow and fast degrees of freedom are well equilibrated. For systems of small molecules the translational degrees of freedom can be easily separated from rotations. We thus define the translational temperature:

$$T_{\mathrm{tr}} = \frac{2}{k(3N-3)}E_{\mathrm{tr}} \tag{29}$$

The number of degrees of freedom is $3N - 3$, taking into account momentum conservation. The rotational temperature is then

$$T_{\mathrm{rot}} = T_{\mathrm{kin}} - T_{\mathrm{tr}}$$

Both temperatures should be the same.

2.8.4. Diffusivity. The diffusivity, as the simplest example of kinetic quantity, was calculated by the Einstein formula from squared displacements averaged over all particles, coordinates, and overlapping blocks 100 ps long with the coverage (overlap) factor three times; correlations of the consecutive data were taken into account in error estimation.[15] First, the dependence of the mean squared displacement on time calculated over shorter blocks and averaged over all simulations was plotted, and the initial nonlinear part determined. For argon we omitted the first 2 ps and for water 20 ps, and the rest was fitted to a linear function. The obtained diffusivity is not corrected for finite size errors.

2.8.5. Gyration Tensor and Shape Anisotropy. Conformation changes of a single molecule can be studied by the gyration tensor and related shape descriptors.[16] We use the mass-weighted tensor:

$$S_{ab} = \frac{1}{M}\sum_i m_i r_{i,a} r_{i,b} \tag{30}$$

where indices a,b run over coordinates x,y,z, index i labels atoms, the atom coordinates are with respect to the center of mass, and $M = \Sigma_i m_i$ is the molecule mass. The radius of gyration is given by the tensor trace, $R_{\mathrm{gyr}}^2 = S_{xx} + S_{yy} + S_{zz}$. To obtain shape descriptors, the tensor must be diagonalized so that in the new coordinates (main axes of inertia) it writes as $S = \mathrm{diag}(\lambda_{xx},\lambda_{yy},\lambda_{zz})$. The relative shape anisotropy κ is then defined by

$$\kappa^2 = \frac{\lambda_{xx}^2 + \lambda_{yy}^2 + \lambda_{zz}^2 - \lambda_{xx}\lambda_{yy} - \lambda_{yy}\lambda_{zz} - \lambda_{zz}\lambda_{xx}}{(\lambda_{xx} + \lambda_{yy} + \lambda_{zz})^2} \tag{31}$$

Note that $0 \le \kappa \le 1$ and that $\lambda_{xx} + \lambda_{yy} + \lambda_{zz} = R_{\mathrm{gyr}}^2$ because of trace invariance.

3. NUMERICAL TESTS

3.1. Ring of Oscillators. The first testing system is small—a ring of $N = 6$ particles of unit mass in one direction. The neighboring particles interact via either harmonic or anharmonic terms:

$$U_{\mathrm{h}}(r) = Kx^2/2$$
$$U_{\mathrm{a}}(r) = K(x^2/2 + x^4/4)$$

where K is the force constant. We used values $K_{i,i+1} = (N + i)/N$, where $i = 0, ..., 5$ and $i = 6$ is identical to 0 so that a ring is created. The momentum is conserved; since the numerical noise becomes detectable in long runs, we reset the total momentum to zero after every integration step. The number of degrees of freedom is $f = N - 1$.

For each method we ran three numerical tests with time steps of $h = 1/16$, $1/32$, and $1/64$, and the correlation time $\tau = 0.3$; in addition, results for $\tau = 0.2$ and 0.5 are presented in the Supporting Information. Each run lasted 2^{25} time units.

The inspection of trajectories shows that the harmonic oscillator simulations exhibit rather poor ergodicity. It is not surprising because this system is similar to the path-integral molecular dynamics, which is known to require a Nosé—Hoover chain for ergodic thermostatting. Both harmonic and anharmonic simulations with the longest time step using a predictor also for energy (eq 15) are unstable and crash with infinite values. The MTTK methods are more (but not 100%) prone to bad ergodicity. Better time reversibility and longer τ improve ergodicity.

The drift in the total energy is shown in logarithmic scale (as $\log_{10}|E_{\mathrm{drift}}|$) in Figure 1. The drift diminishes if: (i) the time step decreases, (ii) the predictor length or the number of iterations increases, and also (iii) τ increases (see the Supporting Information). The TRVP and iteration methods are similar if we use a sufficient predictor length or equivalently increase the number of iterations (increasing the predictor length as well as the number of iterations by 1 decreases the irreversibility error by $\mathcal{O}(h^2)$). The MTTK method is uniformly good even for the longest time steps where the above methods may be unstable. The original Trotter-based version with sym = exp is the best for the harmonic oscillators but worst for the anharmonic ones. The Gear method exhibits the biggest drift, especially for the anharmonic oscillators. We should, however, bear in mind that the drift is only a control quantity and never a final result of interest.

The averaged kinetic temperature (see the Supporting Information) equals the nominal thermostat value with a better precision than the estimated statistical uncertainty for all methods using the same single kinetic temperature in the right-hand side, namely TRVP, iteration, and Gear methods. The original MTTK method, eq 21, gives the average temperature distinguishable from the nominal value only for the longest time step. The modified MTTK methods, eqs 22 and 23, lead to second-order differences; the biggest difference of 0.0025 for $h = 1/16$ and $\tau = 0.2$ drops to 2.5×10^{-5} for $h = 1/64$ and $\tau = 0.5$.

The variance of temperature is $\mathrm{var}T_{\mathrm{kin}} = 0.4$ for both oscillator rings. The results are shown in Figure 2 along with standard errors (68% confidence level) estimated from blocks. The iteration method with only two iterations fails to yield the canonical distribution at all, the longest-time step version fails even with four iterations (whereas three iterations give satisfactory results); however, the fully iterated version is satisfactory. The Gear method does not give the canonical distribution either. The predictor method is slightly better, and the longer predictor results are satisfactory. The MTTK method is uniformly good. The results are much better for the more ergodic anharmonic ring, unless the time step is too long and at the same time the reversibility poor. The best results are for the MTTK method and iterations with the HA kinetic energy, then for predictions with the VV kinetic energy. The Gear method converges poorly and needs a short time step.

As seen from Figure 3, the kurtosis is sensitive to ergodicity problems. For the more ergodic anharmonic oscillator, the MTTK method works well for all time steps, the TRVP method needs $k \geq 2$, and the iteration method $i = 3$ or more iterations to converge well. Different velocity definitions give results differing in the second-order term. Particularly, the LF kinetic temperature but VV velocity is the best with the TRVP method.

The potential energy (see the Supporting Information) gives similar results. The harmonic results are scattered witnessing about poor ergodicity. The MTTK method works well, and the

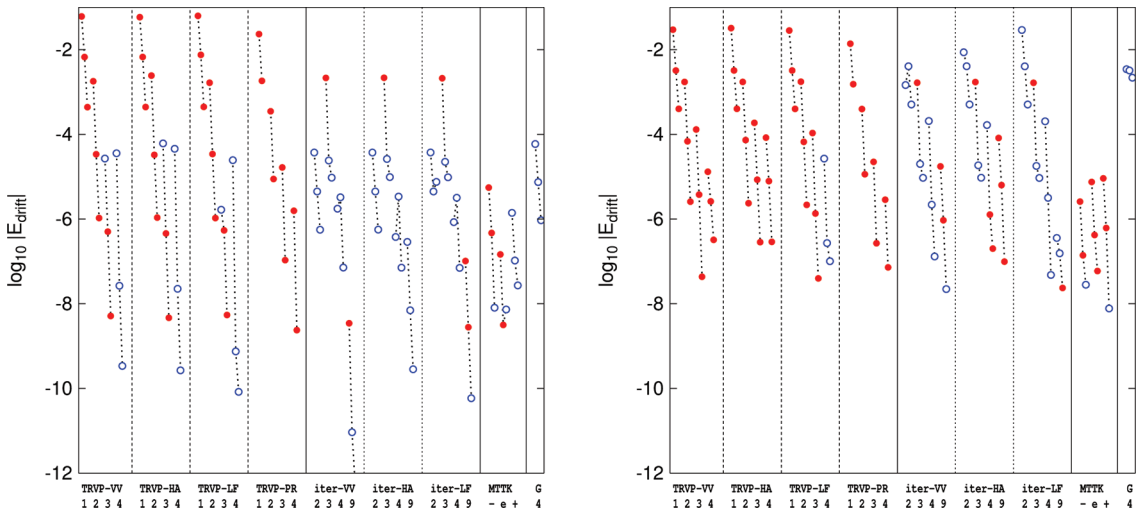

Figure 1. The drift in the total energy (as logarithm of absolute value; negative drifts are open blue circles, positive solid red) for a ring of harmonic (left) and anharmonic (right) oscillators integrated by various methods. The triplets connected by dotted lines are from left for time steps 1/16, 1/32, and 1/64 time units (if the simulation with 1/16 failed, only a doublet is shown). Label 'TRVP' denotes the proposed Nosé—Hoover integration with velocity predictor, the numbers below denote the value of k. Label 'iter' denotes the iteration method (Version 1), the numbers below denote the number of iterations. Symbols 'VV', 'HA', 'LF', and 'PR' refer to the kinetic temperature version, eqs 15 and 18—20. MTTK is the Martyna et al.[5] method, and the symbol below defines function sym(), eqs 21—23. Label 'G' denotes the Gear method ($m = 4$). Error bars are not shown for clarity, they become apparent for $|E_{\mathrm{drift}}| < 10^{-8}$.

dx.doi.org/10.1021/ct200108g |J. Chem. Theory Comput. 2011, 7, 3596–3607

TRVP and iteration methods need several iterations or a longer predictor and are not reliable with long time steps. The anharmonic case, more similar to a typical many-particle atomistic simulation, shows a clearer picture—the systems are ergodic. The best results are obtained with the LF formula for the kinetic energy. The iteration method is the best, followed by the predicted velocities (with $k \geq 2$) and then the MTTK methods.

3.2. Liquid Argon. The second testing system is liquid argon modeled by the Lennard-Jones potential with parameters ε/k = 119.8 K and σ = 3.405 Å. The simulated temperature was 143.76 K (reduced temperature 1.2) and density 1.3443 g cm^{-3} (reduced number density 0.8). We used N = 200 atoms in the standard periodic cubic box, smooth potential cutoff C_2 = 10 Å, time steps h = 20, 10, and 5 fs, and τ = 0.1 ps; more results with τ = 0.3 and 0.5 ps are presented in the Supporting Information. Trajectory length of each point was 200 ns.

We compare the propose predictor method with the iteration method controlled by the error limit in velocity of 10^{-6} reduced units per particle, the Gear integrator (m = 4), and also the Berendsen thermostat (with both the Verlet integrator as well as Gear).

Figure 4 collects the basic thermodynamic results—internal energy and pressure. Error bars were omitted because they are comparable to symbol sizes. It is seen that all methods converge well, however, using the LF kinetic temperature gives the best results, even better than the MTTK method. This observation applies to all methods (TRVP, iterations as well as Gear and also the Berendsen thermostat). The Gear values are shifted because of the finite-size ensemble error; this difference will diminish for larger systems. The TRVP method with the shortest predictor k = 1 is sufficient; only if the kinetic energy was calculated from the predicted velocities (version PR), a longer predictor would be needed, but this version is not recommended anyway.

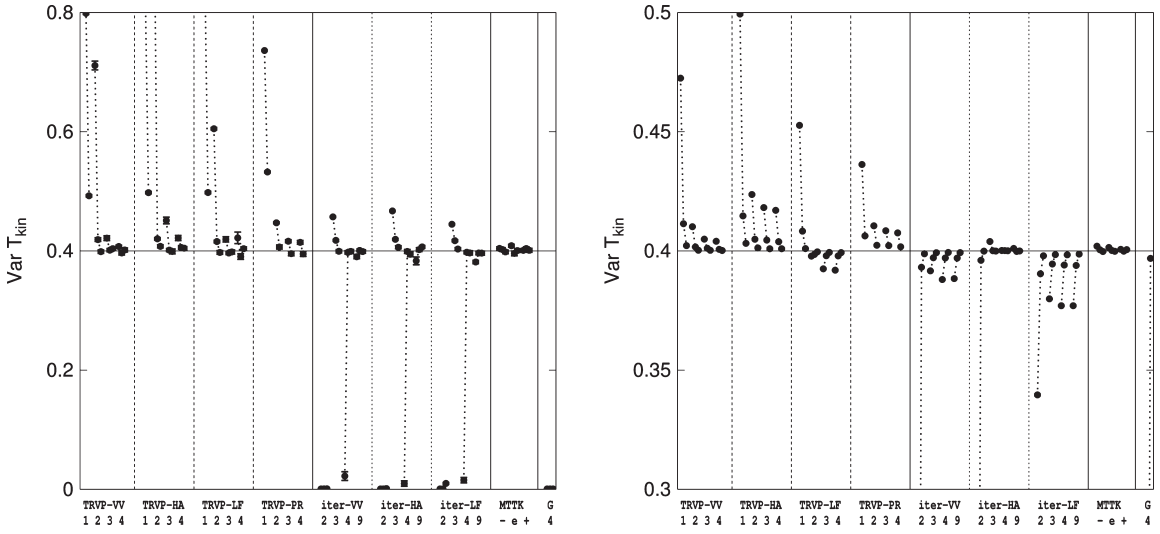

Figure 2. The variance of temperature for a ring of oscillators. See Figure 1 for symbol explanation. Note the different scales of the vertical axes.

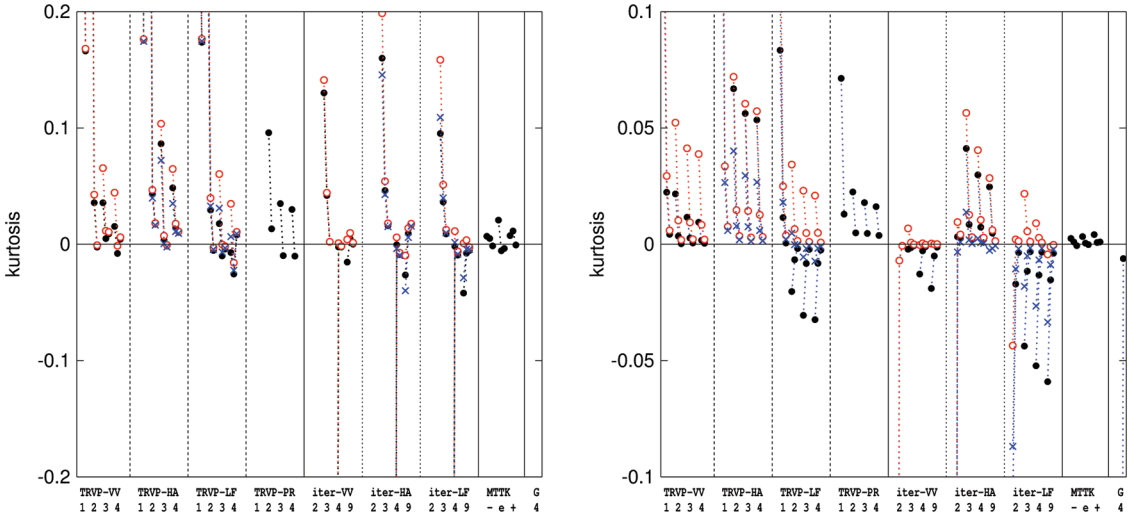

Figure 3. Kurtosis of the velocity distribution averaged over all 6 oscillators. Left: harmonic, right: anharmonic. Black solid circles: "natural" velocity, red open circles: single leapfrog velocity $[r(t) - r(t-h)]/h$, blue cross: VV ($[r(t+h) - r(t-h)]/(2h)$), if differs from the "natural" velocity. See Figure 1 for symbol explanation. Note the different scales of the vertical axes.

Figure 5 shows, along with the temperature variance, also kurtosis of the distribution of velocities; note that the kurtosis is calculated from the "natural" velocity definition for the TRVP method (see Section 2.8.3), whereas from the VV formula for iterations. It is seen that all the Nosé−Hoover methods converge to the correct values (at least within error bars, which are for the variance several symbol sizes). The Berendsen values are out of the graph because this method is not canonical. The TRVP method gives better temperature variance with $k = 2$ than $k = 1$, however, increasing the predictor length to $k > 2$ gives only a marginal improvement. The MTTK results are the best even for large time steps. The VV velocity (eq 18) works best with TRVPs while the HA velocity (eq 19) with iterations.

The results for diffusivity, Figure 6, are subject of larger errors than for mechanical quantities. All methods and both thermostats converge well, only the TRVPs with the harmonic and predicted temperatures perform worse with long time steps. Both the TRVPs and iterations with the VV and LF temperatures are acceptable. Surprisingly, the Gear integration (both with the Nosé−Hoover and Berendsen thermostats) wins the comparison.

3.3. Liquid Water. The third testing system consists of $N = 200$ SPC/E[13] water molecules in a cubic box simulated at ambient conditions (density 997 kg m^{-3}, temperature 300 K). Both the Lennard-Jones and electrostatics cutoffs were set to $C_2 = 9$ Å. We further utilized $h = 2$, 1, and 0.5 fs and $\tau = 0.1$ ps, and the runs took 50 ns. Selected results

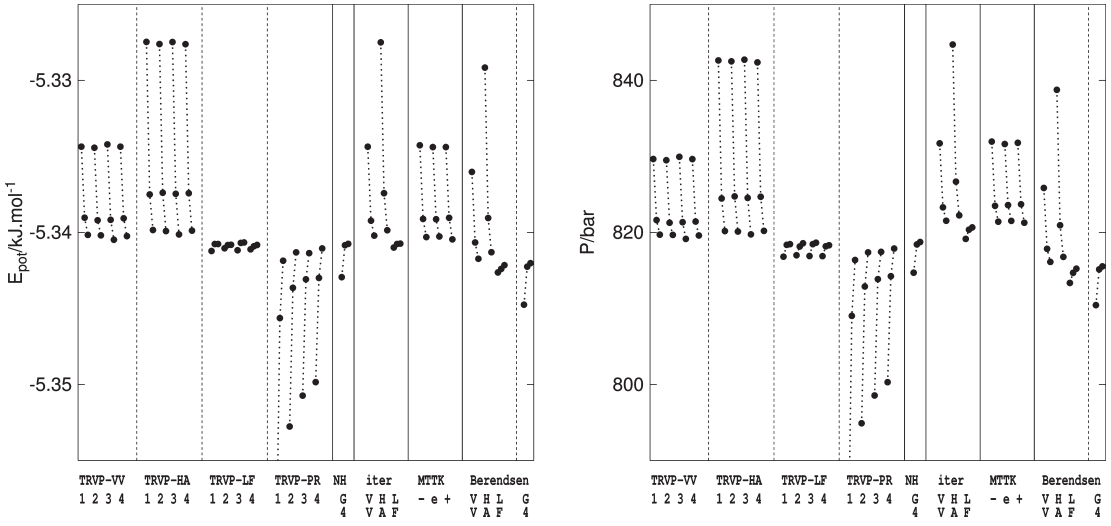

Figure 4. Averaged potential energy (left) and pressure (right) for liquid argon. The triplets connected by dotted lines correspond (from left) to time steps 20, 10, and 5 fs. Label 'TRVP' denotes the proposed Nosé−Hoover integration with velocity predictor, the numbers below denote the value of k. Label 'iter' denotes the iteration method (Version 2) with the number of iterations controlled by precision. Symbols 'VV', 'HA', 'LF', and 'PR' refer to the kinetic temperature version. MTTK is the Martyna et al.[5] method and the symbol below defines function sym(), eqs 21−23. Label 'G' denotes the Gear method ($m = 4$), either with Nosé−Hoover (NH) or Berendsen thermostat. Error bars are comparable to symbol sizes.

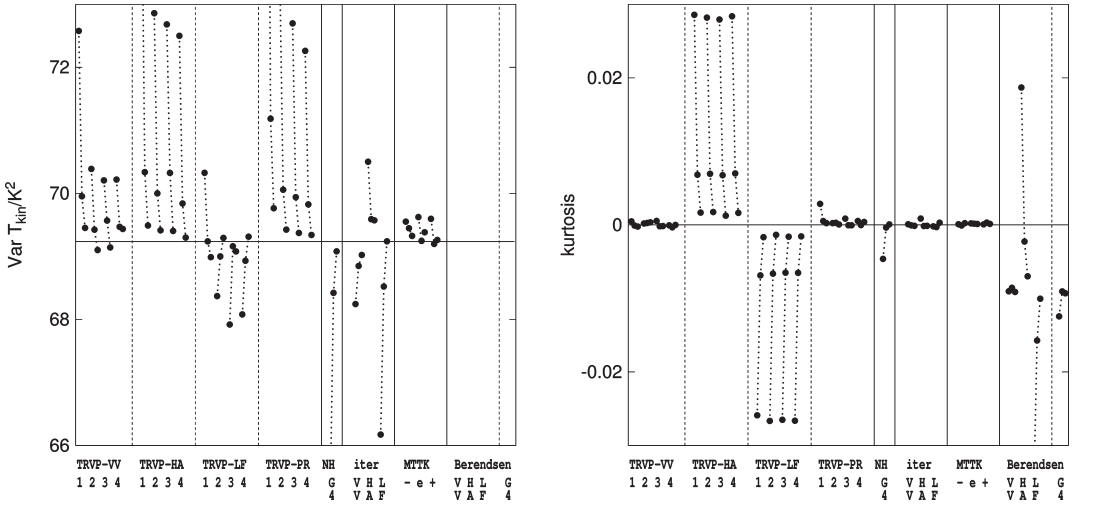

Figure 5. Variance of temperature and kurtosis of the velocity distribution for liquid argon. The horizontal lines represent the respective theoretical values. See Figure 4 for symbol explanation.

dx.doi.org/10.1021/ct200108g |J. Chem. Theory Comput. 2011, 7, 3596–3607

with τ = 0.3 and 0.5 ps are presented in the Supporting Information.

The results for the potential energy, Figure 7, are similar as for argon: the TRVP and iteration methods are equivalent. It is more important to choose the kinetic energy formula. The LF version is the best, the VV version is worse and of the same accuracy as the MTTK method (using internally the same velocity approximation). The Gear integrator performs surprisingly well.

The results for pressure are different, for TRVPs (and also Berendsen thermostat) the VV kinetic temperature overperforms the LF one. However, this result can be explained by a "dynamic" atom-based algorithm, eq 25, used here for pressure. Of course, both formulas give results differing by a term proportional to h^2.

The variance of temperature, Figure 8, is in spite of 50 ns runs and a relatively small system, a subject of large errors. Essential all methods, perhaps with the exception of the harmonic approximation for the kinetic temperature (and of course the Berendsen thermostat), give satisfactory results. The kurtosis is worse for the HA and LF temperatures and long time steps.

The equipartition of translational and rotational kinetic energies, Figure 9, depends on the time step and the kinetic temperature formula, but not on the integration method: the LF version is the best, followed by VV, whereas HA and PR are not so good. The diffusivity, Figure 10, behaves in the same way, only the data are more noisy. To a great extent also the potential energy and (with the "static" eq 26) also pressure follow the same pattern. This observation is not surprising because most thermostats keep the averaged (translational and rotational) temperature constant, whereas the Verlet integration errors increase the translational temperature. The center-of-mass velocities are then bigger, and the diffusivity increases. Similarly, the energy and pressure depend mainly on the interparticle energy. One may ponder that Nosé−Hoover and Berendsen thermostats with only the translational kinetic energy could give (some) thermodynamic quantities more accurately.

3.4. Peptide. As the last testing system we chose a small peptide in vacuum, hexaalanine modified by acetyl at the N-terminus and *N*-methylamide at the C-terminus (CH_3−CO−[NH−$CHCH_3$−CO]$_6$−NH−CH_3) because: (i) a complex set of bonds provides a comprehensive test of constraint dynamics; (ii) it has a sufficiently rich conformational space to check for possible ergodicity problems; and (iii) a relatively small number of atoms facilitates sampling of all important conformations. The molecule was modeled by the GROMOS96[17] force field version 43A1 (with united-atom approximation for the CH_3 and CH groups). However, for simplicity of coding we did not apply nonbonded fixes (exceptions) for 1−4 nonbonded interactions and included them in full. This change has a minor impact on the peptide properties. We also replaced the torsion term around the peptide bond by a locally equivalent harmonic potential and prohibited thus the cis conformations at all, because in trial runs with the original dihedral potential, we detected the trans−cis conversion at a hundred

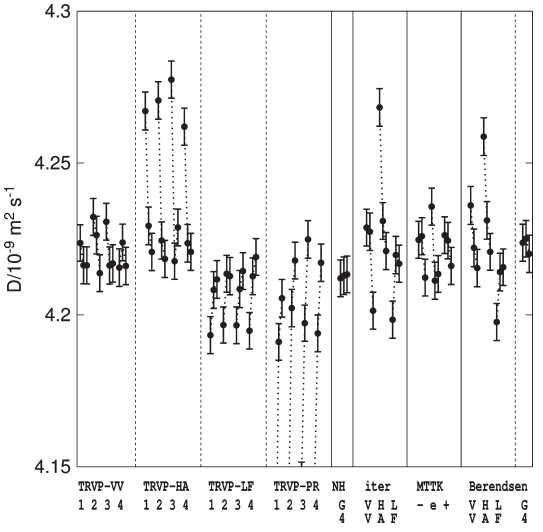

Figure 6. Diffusivity of liquid argon. See Figure 4 for symbol explanation. The error bars denote estimated standard errors.

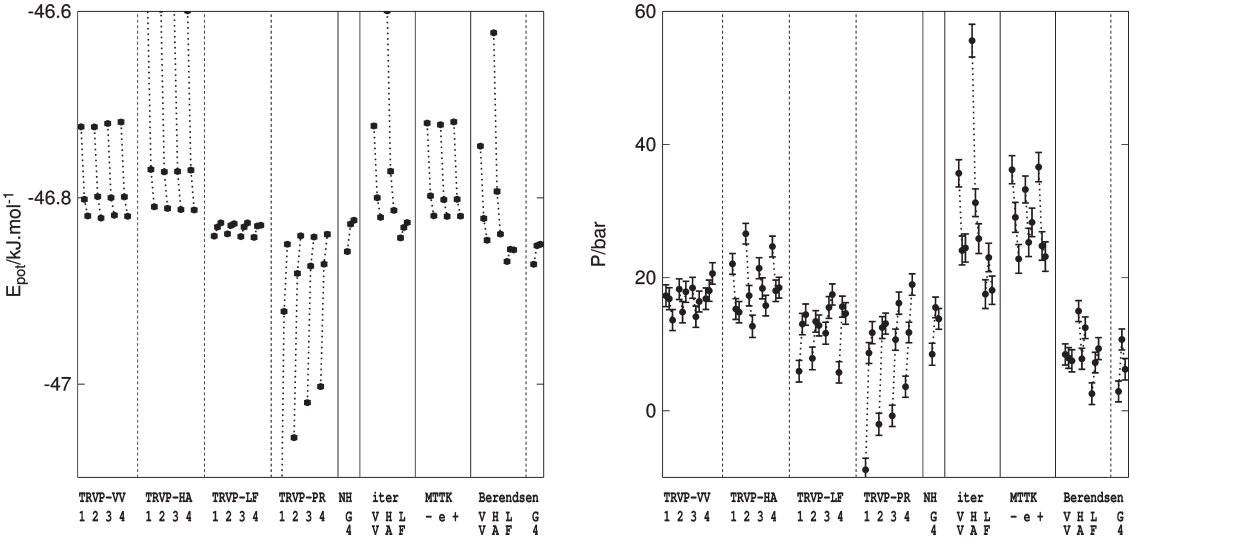

Figure 7. Averaged potential energy (left) and pressure (right) for liquid SPC/E water. The triplets correspond to time steps of 2, 1, and 0.5 fs, for other symbols see Figure 4.

dx.doi.org/10.1021/ct200108g |*J. Chem. Theory Comput.* 2011, 7, 3596–3607

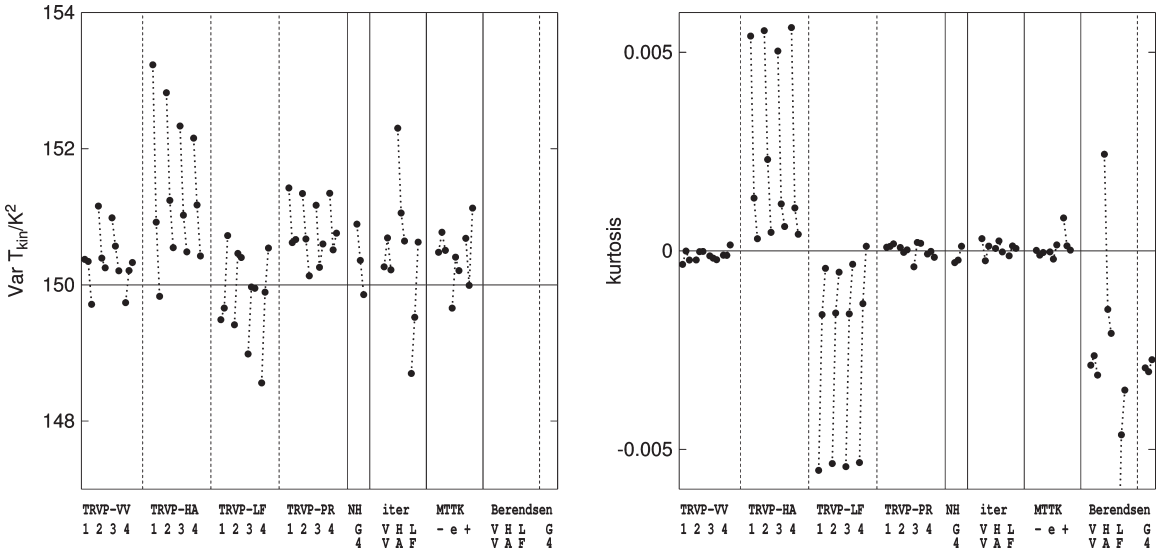

Figure 8. Variance of temperature and kurtosis of the velocity distribution for liquid water. The horizontal lines represent the theoretical values. See Figure 7 for symbol explanation.

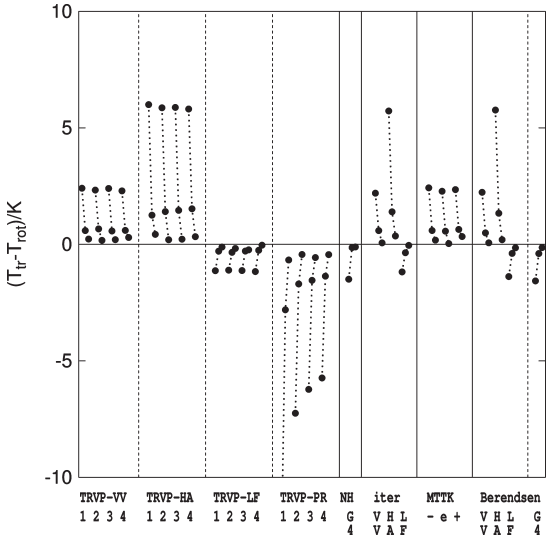

Figure 9. Equipartition of the translational and rotational temperatures for liquid water. See Figure 7 for symbol explanation.

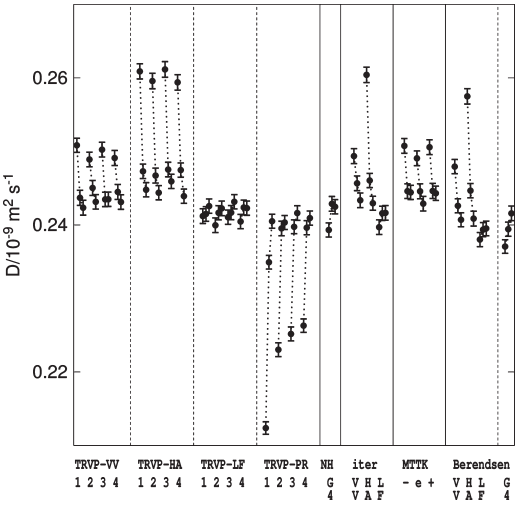

Figure 10. Diffusivity of liquid water. See Figure 7 for symbol explanation. The error bars denote estimated standard errors.

nanosecond scale, which spoiled the statistics. Note that our aim is not to obtain an accurate realistic representation of this peptide but a model system reasonably close to realistic biomolecules, yet simple enough to allow for accurate comparison of methods.

The peptide with constrained bond lengths was simulated at 450 K for 1 μs using three time steps and the Nosé−Hoover or Berendsen correlation times of τ = 0.1 ps. The TRVP method and Berendsen thermostat were implemented using MACSIMUS,[11] for the iterated velocity, and for the MTTK method we used DL_POLY;[12] only the VV version of the kinetic temperature, eq 18, and the original MTTK method are available. The momentum and angular momentum were periodically reset to exact zero and do not contribute to the number of degrees of freedom.

The internal energy is the least noisy variable of interest, see Figure 11 left. All canonical methods converge as the time step decreases, whereas the Berendsen value is off as expected for this small system of only 79 degrees of freedom. The leapfrog version of the kinetic energy definition is again the best.

The variance of temperature, see Figure 11 right, converges to the correct value similarly as for other investigated systems; because of a small number of degrees of freedom, the results are less noisy than for liquids. The values for the noncanonical friction thermostat are off the graph scale.

The averaged radius of gyration and averaged shape anisotropy show a similar pattern of convergence as the potential energy; only the data are more noisy (Figure 12). The TRVP method with both major kinetic energy definitions, VV and LF, performs well even for the longest time step and so do the benchmark methods, iterations (with VV), and MTTK. The Gear integrator is satisfactory with the shortest time step only.

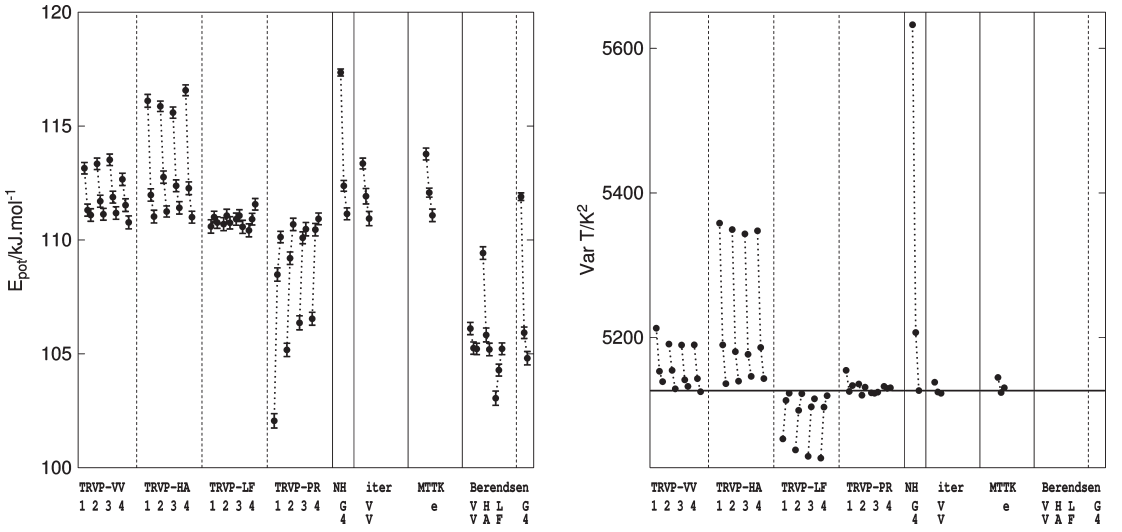

Figure 11. Averaged potential energy (left) and variance of temperature (right) for modified hexaalanine in vacuum at 450 K. The triplets correspond to time steps of 2, 1, and 0.5 fs, for other symbols see Figure 4. The horizontal line is the theoretical value of temperature variance, eq 28.

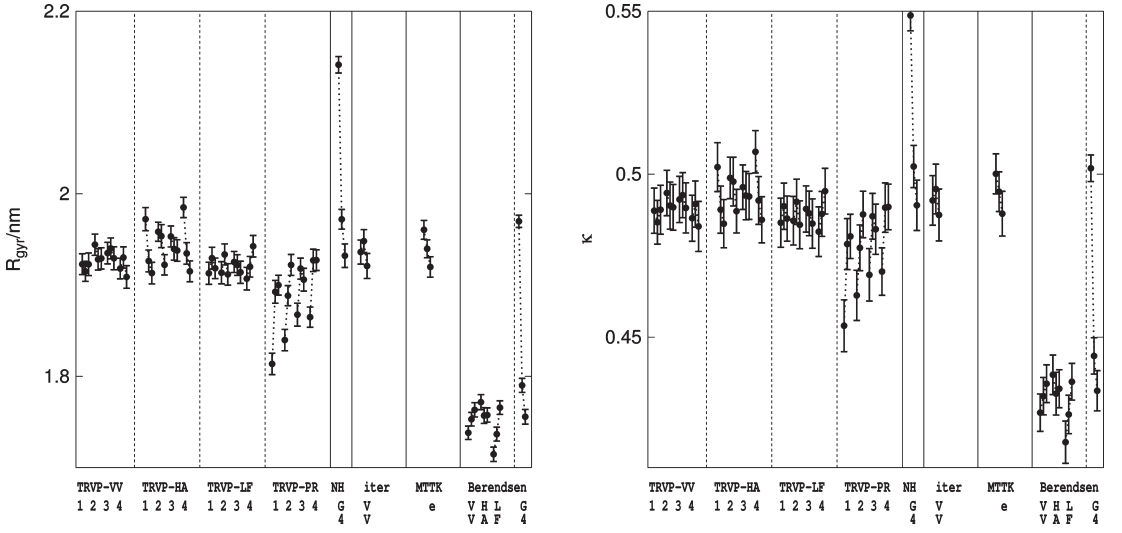

Figure 12. Radius of gyration (left) and relative shape anisotropy κ (right) for modified hexaalanine in vacuum at 450 K. The triplets correspond to time steps of 2, 1, and 0.5 fs, for other symbols see Figure 4.

4. CONCLUSIONS

4.1. TRVP Method. The proposed TRVP method, see Section 2.6, is the main result of this work. It has been successfully applied to the Nosé−Hoover thermostat and Verlet integrator for many-particle atomistic systems, including those with constrained bond lengths. The method quality and speed are similar to the iteration method, and the decision which method to use may thus rather depends on algorithm subtleties. The TRVP method can be coded outside the existing Verlet + SHAKE algorithm, which may simplify the code design. Only one set of SHAKE iterations is needed, and thus measuring some quantities (e.g., the pressure tensor) does not interfere with repeated calculations. On the other hand, the TRVP method requires more memory than the iteration method. Often the shortest predictor ($k = 1$) is sufficient, although $k = 2$ is never worse.

The MTTK method is for large atomistic systems comparable to both the above simple Verlet-based methods. As it is more complex, the kinetic energy is calculated four times per step, and for constrained systems it requires the RATTLE algorithm that is more CPU consuming than the SHAKE algorithm. For small systems, it performs better than both the TRVPs and iterations, avoiding many ergodicity problems; on the other hand, it is slower.

4.2. Velocity Estimates in Verlet Schemes. The TRVP and iteration methods are of the second order in the time step. At the same time there are several formulas, eqs 15 and 18−20 available to approximate velocities and in turn the kinetic temperature. They yield different coefficients at the second-order error terms for different quantities. We found that the LF eq 20 gives the overall best results for quantities of interest (energy, pressure, diffusivity), although the quality of the canonical distribution is worse. The method accuracy may depend on the details of the algorithm, e.g., an atom-based formula for pressure for constrained systems is better with the VV kinetic energy, eq 18,

probably because this formula depends on the constrained forces, which depend on velocities.

4.3. Modification of MTTK Algorithm. We proposed two modifications of the MTTK algorithm, see eqs 22 and 23, which avoid evaluating the exponential functions and therefore run faster. The speedup is insignificant for large atomistic systems but may be worth considering in some special cases, like Nosé−Hoover chains for simple systems. The kinetic temperature derived from the velocities available within the algorithm is (inconsistently) off by a second-order term in the time step, however, other observable quantities are not affected. One might consider alternating sym_+ and sym_- in the Nosé−Hoover chain in order to decrease the kinetic temperature error. Compromise functions sym() better approximating exp() than eqs 22 and 23 are also possible.

4.4. Translational Temperature. In the simulations of liquid water we found that the values of many quantities (energy, pressure, diffusivity) depend mainly on the translational temperature, eq 29. Using this temperature in the thermostat may compensate for large time step errors of the Verlet integration. A similar correction for equipartition errors might be possible for the internal vibrations instead of rotations.

■ ASSOCIATED CONTENT

Supporting Information. Extended sets of results are available: runs with different correlation times τ (except for the peptide); more quantities (e.g., the kinetic temperatures, electrostatic energy for water); time profiles of the total energy for the ring of oscillators; and more shape descriptors, the end-to-end distance, and correlation times for the model peptide. This material is available free of charge via the Internet at http://pubs.acs.org.

■ AUTHOR INFORMATION

Corresponding Author
*E-mail: jiri.kolafa@vscht.cz.

■ ACKNOWLEDGMENT

This work was supported by the Czech Science Foundation, projects P208/10/1724 (J.K.) and 104/08/0600 (M.L.) and the Internal Grant Agency of the J. E. Purkinje University, grant no. 53222 15 0006 01 (M.L.).

■ REFERENCES

(1) Allen, M. P.; Tildesley, D. J. *Computer Simulation of Liquids*; Clarendon Press: Oxford, U.K., 1986.
(2) Frenkel, D.; Smit, B. *Understanding Molecular Simulation*; Academic Press: San Diego, CA, 2002.
(3) Ralston, A. *A First Course in Numerical Analysis*; McGraw-Hill: New York, 1965.
(4) Gear, C. W. *Numerical Initial Values Problems in Ordinary Differential Equations*; Prentice Hall: Upper Saddle River, NJ, 1971.
(5) Martyna, G.; Tuckerman, M. E.; Tobias, D. J.; Klein, M. L. *Mol. Phys.* **1996**, *87*, 1117–1157.
(6) Toxvaerd, S. *Mol. Phys.* **1991**, *72*, 159–168.
(7) Nosé, S. *Mol. Phys.* **1984**, *52*, 255–268.
(8) Hoover, W. G. *Phys. Rev. A* **1985**, *31*, 1695–1697.
(9) Kolafa, J. *J. Comput. Chem.* **2004**, *25*, 335–342.
(10) de Leeuw, S. W.; Perram, J. W.; Petersen, H. G. *J. Stat. Phys.* **1990**, *61*, 1203–1222.
(11) *MACSIMUS*; Institute of Chemical Technology: Prague, Czech Republic, 2011; http://www.vscht.cz/fch/software/macsimus, (accessed Aug 19, 2011).
(12) Todorov, I.; Smith, W. *The DL POLY 3 User Manual*; STFC Daresbury Laboratory: Cheshire, U.K., 2009.
(13) Berendsen, H. J. C.; Grigera, J. R.; Straatsma, T. P. *J. Phys. Chem.* **1987**, *91*, 6269–6271.
(14) Kolafa, J.; Moučka, F.; Nezbeda, I. *Collect. Czech. Chem. Commun.* **2008**, *73*, 481–506.
(15) Picálek, J.; Kolafa, J. *J. Mol. Liq.* **2007**, *134*, 29–33.
(16) Mattice,W. L.; Suter, U. W. *Conformational Theory of Large Molecules*;Wiley Interscience: Hoboken, NJ, 1994.
(17) van Gunsteren, W. F.; Billeter, S. R.; Eising, A. A.; Huenenberger, P. H.; Krueger, P.; Mark, A. E.; Scott, W. R. P.; Tironi, I. G. *The GROMOS96 Manual and User Guide*; BIOMOS: Zurich, Switzerland, 1996.